Virus Research 155 (2011) 462–472

Contents lists available at ScienceDirect

Virus Research

journal homepage: www.elsevier.com/locate/virusres

Analysis of SAT1 type foot-and-mouth disease virus capsid proteins: Influence of receptor usage on the properties of virus particles

Francois F. Maree[a,*], Belinda Blignaut[a,b], Lisa Aschenbrenner[c], Tom Burrage[c], Elizabeth Rieder[c]

[a] Transboundary Animal Diseases Programme, Onderstepoort Veterinary Institute, Agricultural Research Council, Old Soutpan Road, Onderstepoort, Pretoria 0110, South Africa
[b] Department of Microbiology and Plant Pathology, Faculty of Agricultural and Natural Sciences, University of Pretoria, Pretoria 0002, South Africa
[c] Foreign Animal Disease Research Unit, United States Department of Agriculture, Agricultural Research Service, Plum Island Animal Disease Center, Greenport, NY 11944, United States

ARTICLE INFO

Article history:
Received 12 August 2010
Received in revised form 6 December 2010
Accepted 9 December 2010
Available online 15 December 2010

Keywords:
Foot-and-mouth disease virus
Infectious cDNA
Recombinant virus
Integrin receptor
Heparan sulphate proteoglycan

ABSTRACT

The three SAT serotype viruses, endemic in Africa, are well known for their difficulty to adapt to cell culture. The viral mechanism involved in foot-and-mouth disease virus (FMDV) tissue tropism and cell-entry is not well understood. A recombinant, small plaque-forming virus (vSAT1tc), derived from a tissue culture-adapted SAT1 virus (SAR/9/81tc), revealed four amino acid substitutions (VP3 Asp192 → Tyr; VP3 Ser217 → Ile; VP1 Ala69 → Gly and VP1 Asn110 → Lys) in the capsid, compared to the SAR/9/81wt isolate collected from infected impala epithelium. One substitution added a positively charged lysine residue to the short βF-βG loop of VP1. Furthermore, vSAT1tc displayed a high affinity for CHO-K1 cells possibly via interaction with negatively charged sulphated polysaccharides while SAT1 impala strain relied strongly on $\alpha_V\beta6$ integrin receptors for cell entry. The cell culture adaptation and small plaque phenotype of vSAT1tc was accompanied by differences in particle aggregation and significant differences in acid stability. Based on limited cross neutralization data, the antigenic features seem to be unchanged. Thus, acquisition of positively charged residues in the virion may be beneficial for adaptation of SAT type field strains to cell culture.

1. Introduction

Foot-and-mouth disease (FMD) is a highly contagious, vesicular disease affecting primarily cloven-hoofed animals with severe economic consequences worldwide (Bachrach, 1968; Sutmoller, 2003). Although mortality is usually low, morbidity can reach 100% and causes severe losses in production. Therefore, the disease remains a major economic concern for livestock-health in many developing countries and a continued threat to disease-free countries (Knowles & Samuel, 2003; Vosloo et al., 2003). The causative agent, FMD virus (FMDV), is the prototype species of the *Aphthovirus* genus within *Picornaviridae* and seven distinct serotypes, *i.e.* A, O, C, South African Territories (SAT) types 1–3 and Asia-1, are distinguished. With the exception of Asia-1, all the remaining serotypes have been isolated on the African continent, while the three SAT types are located almost exclusively in sub-Saharan Africa (Vosloo et al., 2001). The SAT types display large genetic (Vosloo et al., 1995; Van Rensburg and Nel, 1999; Bastos et al., 2001, 2003a,b) and antigenic variability (Esterhuysen et al., 1988; Parry et al., 1990), as well as regional differences in the distribution and prevalence of serotypes. These types are further characterised by their ability to infect multiple wildlife hosts.

African buffalo (*Syncerus caffer*) in southern Africa have been shown to be persistently infected with the SAT type viruses (reviewed in Thomson et al., 2003) and are an important source of infection for domestic animals (Dawe et al., 1994; Bastos et al., 1999). Buffalo are rarely clinically affected by FMD, but act as carriers of the disease with virus transmitted from adult to young animals (Thomson et al., 1992; Vosloo et al., 1996). Since 2000, various outbreaks of FMD were recorded in vaccinated cattle populations in southern Africa where, in many cases, the source of virus was traced to buffalo. Although SAT2 type virus is the causative agent in most outbreaks of FMDV in cattle in sub-Saharan Africa (ca. 60% of outbreaks), SAT1 is widely dispersed and are mostly maintained through persistent infections of African buffalo (ca. 55% of buffalo isolates), whereas SAT3 has the lowest incidence level (Heath, 2008).

In endemic regions, FMD is controlled by restricting animal movement, the implementation of vaccination programmes and hygienic measures. Current FMD vaccines are chemically inactivated preparations of concentrated, virus infected cell

Abbreviations: FMD, foot-and-mouth disease; FMDV, FMD virus; GAG, glycosaminoglycan; HSPG, heparan sulphate proteoglycan; SAT, South African Territories.

* Corresponding author. Tel.: +27 12 529 9584/93; fax: +27 12 529 9595/05.
E-mail address: mareef@arc.agric.za (F.F. Maree).

0168-1702/$ – see front matter © 2010 Elsevier B.V. All rights reserved.
doi:10.1016/j.virusres.2010.12.002

culture supernatants (Office International des Épizooties Terrestrial Manual, 2009) and require that the vaccine strain is adapted and propagated in cell culture (Amadori et al., 1994, 1997). This necessitates continuous adaptation of new vaccine strains to cell culture whenever a close antigenic relationship to an outbreak virus is required. It is thought that adaptation to cell culture is made possible by the selective pressure exerted by the cell surface molecules, which may act as virus receptors for viral quasi-species (Baranowski et al., 1998). However, it has been noted that SAT viruses are difficult to adapt to BHK-21 cells to enable large scale propagation (Pay et al., 1978; Preston et al., 1982).

Two classes of cell surface receptors that mediate FMDV infection have been identified *in vitro*. FMDV enters cultured cells by binding to any of four members of the integrin family of cellular receptors ($\alpha_V\beta1$, $\alpha_V\beta3$, $\alpha_V\beta6$ and $\alpha_V\beta8$) or to heparan sulphate proteoglycans (HSPG; glycosaminoglycans or GAG's) (Berinstein et al., 1995; Sa-Carvalho et al., 1997; Duque & Baxt, 2003; Jackson et al., 1996, 2000, 2002, 2004; Neff et al., 1998, 2000; Neff and Baxt, 2001). FMDV attachment to integrin receptors occurs via a highly conserved arginine–glycine–aspartic acid (RGD) tripeptide motif, which is located on the flexible, surface-exposed βG-βH loop of VP1 (Pfaff et al., 1988; Surovoĭ et al., 1988; Fox et al., 1989; Baxt & Becker, 1990; Logan et al., 1993; Mason et al., 1994; Berinstein et al., 1995). Sequences flanking the RGD motif and the conformation of the βG-βH loop have been shown to influence the specificity of binding to different integrin receptors (Rieder et al., 1993; Duque & Baxt, 2003). Although the integrin $\alpha_V\beta6$ has been shown to act as a high affinity receptor for certain serotypes of FMDV found in cattle-to-cattle transfer (Jackson et al., 2000; Duque & Baxt, 2003; Duque et al., 2004; Monaghan et al., 2005; Burman et al., 2006), very little is known about the virus–host interaction and receptor usage of SAT type viruses maintained in the African buffalo. The ability of FMDV to use HSPG as receptors appears to be restricted to FMDV strains that have frequently been passaged in cultured cell lines (Jackson et al., 1996; Sa-Carvalho et al., 1997).

As a first step towards understanding virus–cell interaction during cell culture-adaptation of SAT viruses we report on amino acid substitutions that are fixed during the adaptation process of a SAT1 virus. The SAT1 virus chosen in this study, caused numerous outbreaks in several wildlife species in the Kruger National Park (KNP) and surrounding area during early 1980s. An isolate from that outbreak, SAR/9/81wt, was adapted to grow in BHK-21 cells and used in the preparation of inactivated vaccine for the control of FMD adjacent to the KNP. SAT1 infectious cDNA clones were constructed from the virus isolated from impala antelope (*Aepecuros melampus*) and its cell culture-adapted derivate. A recombinant, small plaque-forming virus, derived from a tissue culture-adapted SAT1 virus (vSAT1tc), revealed four amino acid substitutions in the capsid compared to the isolate collected from infected impala epithelium. One substitution added a positively charged lysine residue to the short βF-βG loop of VP1 and was found to be associated with adaptation of SAT1 virus to BHK-21 cell cultures. The ability of the cell culture-adapted phenotype to form aggregates and virion stability under different environmental conditions were examined.

2. Materials and methods

2.1. Cells and viruses

Baby hamster kidney (BHK) cells, strain 21, clone 13 (ATCC CCL-10) were maintained as previously described (Rieder et al., 1993) and were used during transfection, virus recovery, plaque assays and one-step infectivity kinetic studies. Plaque assays were also performed using IB-RS-2 (Instituto Biologico renal suino) and Chinese hamster ovary (CHO) cells strain K1 (ATCC CCL-61) maintained in RPMI medium (Sigma) and Ham's F-12 medium (Invitrogen), respectively, supplemented with 10% foetal calf serum (Delta Bioproducts).

The SAT1 virus causing the 1981 outbreak was originally isolated from impala epithelium (SAR/9/81wt; wild-type) and adapted on BHK-21 cells for vaccine production (SAR/9/81tc; passage history PK1RS4BHK5). Viruses were isolated on primary pig kidney cells (PK), followed by 4 passages in IB-RS-2 cells. For serial passages, infected (or transfected) 35-mm-diameter BHK-21 cell monolayers were frozen and thawed and 1/10th of the volume was used to inoculate a fresh monolayer. To determine population quasi-species a serial dilution of SAR/9/81tc virus was prepared in 96-well cell culture plates (Nunc™) and the supernatant of wells containing single foci of infection were used for RNA extraction, RT-PCR and the nucleotide sequence of the VP1-coding region determined.

2.2. RNA extraction, cDNA synthesis, plasmid construction and mutagenesis

RNA was extracted from infected cell lysates using TRIzol® reagent (Life Technologies) according to the manufacturer's specifications and used as template for cDNA synthesis. Viral cDNA was synthesised with SuperScript III™ (Life Technologies) using a poly-dT primer.

Genome-length cDNA clones, carrying the genomic sequences of SAR/9/81wt and SAR/9/81tc, were constructed using a similar cloning strategy to the one employed by Rieder et al. (1993, 2005) and Van Rensburg et al. (2004). The respective plasmids were designated pSAT1wt (a and b) and pSAT1tc. Genomic cDNA was amplified via standard PCR using Advantage™ Taq DNA Polymerase (Clontech) in the presence of genome-specific oligonucleotides tailored with appropriate restriction enzyme recognition sites to allow easy cloning. The 8143 bp SAT1 genomic cDNA was cloned into pGEM plasmid using *Xma*I and *Not*I restriction sites. The nucleotide sequence of the cloned regions was subsequently determined using the ABI PRISM™ BigDye Terminator Cycle Sequencing Ready Reaction Kit v3.0 (Applied Biosystems). The VP3/VP1/2A-coding region of the plasmid pSAT1wt-a was recovered using *SnaBI* and *XmaI* restriction enzymes and cloned into the corresponding region of pSAT1tc, to generate the plasmid pSAT1tc/wt.

Site-directed mutagenesis of plasmid pSAT1tc to produce pSAT1tcK-N was accomplished by an inverse PCR method using the Quick change mutagenesis kit (Stratagene). The forward mutagenesis primer CAGTCGTCTTTTCCAAcgGAGGAGCCACCCGCTTTGC (lower cased letters represent altered bases) replaced the Lys at position 110 of VP1 with the wild-type Asn residue. The mutation was verified by automated sequencing and no unintended site mutations were found.

2.3. In vitro RNA synthesis, transfection and virus recovery

RNA was synthesised from *NotI*-linearised plasmid DNA templates using the MEGAscript™ T7 kit (Ambion). BHK-21 cell monolayers, in 35 mm diameter cell culture plates (Nunc™), were transfected with the *in vitro*-generated RNA using Lipofectamine2000™ (Life Technologies) according to the manufacturer's recommendations. The transfection medium was removed after 3–5 h and replaced with Eagle's basal medium (BME) containing 1% FCS and incubated at 37 °C up to 48 h. After one freeze–thaw cycle the transfection supernatants were used for serial passaging on BHK-21 cells until complete CPE. Unless otherwise stated passage 4 was used for analysis. Viruses recovered from transfection of pSAT1tc, pSAT1wt-a, pSAT1wt-b, pSAT1tcK-N and pSAT1tc/wt were designated vSAT1tc, vSAT1wt-a, vSAT1wt-b, vSAT1tcK-N and vSAT1tc/wt.

2.4. Plaque titrations and growth kinetics

Plaque titrations were performed in BHK-21, IB-RS-2 and CHO-K1 cells, which were infected with the viruses for 1 h, followed by the addition of a 2 ml tragacanth overlay (Rieder et al., 1993). After incubation for 27 or 40 h the infected cell monolayers were stained with 1% (w/v) methylene blue in 10% ethanol and 10% formaldehyde prepared with phosphate buffered saline, pH 7.4.

One-step growth kinetics were carried out in BHK-21 cells which were infected with the viruses at a multiplicity of infection (m.o.i.) of 2–4 PFU/ml for 1 h, washed with MBS-buffer (1 M MES, 1.45 M NaCl, pH 5.5) prior to incubation at 37 °C for the indicated time interval, harvested at 2, 4, 6, 8, 10, 12, 16 and 20 h post-infection and frozen at −70 °C. Virus titres were determined on BHK-21 cells and expressed as the logarithm of the plaque forming units per millilitre (PFU/ml).

2.5. Virus neutralization (VN) test

The antigenic diversity of the SAR/9/81wt, SAR/9/81tc and vSAT1tc viruses was determined using the micro-neutralization test carried out as described in the OIE Manual of Standards (2009) with reference cattle sera prepared by two consecutive vaccinations (vaccinated at day 0, boosted at day 28 and bled at day 38) with the homologous SAR/9/81tc, and heterologous SAT1/KNP/196/91 and SAT1/NIG/5/81 vaccines. IB-RS-2 cells were used as the indicator system in the neutralization test. The end point titre of the serum against homologous (SAR/9/81wt, SAR/9/81tc and vSAT1tc) and heterologous (SAT1/KNP/196/91 and SAT1/NIG/5/81) viruses was calculated as the reciprocal of the last dilution of serum to neutralise 100 $TCID_{50}$ in 50% of the wells (Rweyemamu, 1978). One-way antigenic relationships (r1-values) of the field isolates and engineered viruses relative to the reference sera were calculated, which is expressed as the ratio between the heterologous/homologous serum titre. All neutralization titre determinations were repeated at least twice.

2.6. Analysis of receptor usage of the SAT1 viruses

Cell-binding studies were essentially performed as described by Neff et al. (2000) and Duque and Baxt (2003). This entails the infection of COS-1 cells, transiently expressing the bovine integrin α_V subunit and either the β1, β3 or β6 subunits, with the SAR/9/81wt or vSAT1tc viruses, respectively. Sixteen hours after infection, cells were labelled with [^{35}S]methionine and viral protein synthesis analyzed by radio-immunoprecipitation (RIP) of equal amounts of trichloroacetic acid-precipitable counts per minute using a SAT1 polyclonal serum followed by sodium dodecyl sulphate-polyacrylamide gel electrophoresis (SDS-PAGE). Radio-labelled proteins from non-transfected COS-1 cells and BHK-21 cells infected with SAR/9/81wt were included as controls.

Twenty-four hours growth study was performed in CHO-K1 cells which express GAG receptors (Jackson et al., 1996; Sa-Carvalho et al., 1997) and CHO-677 (deficient in GAG expression). Monolayer cells in 35 mm cell culture plates (Nunc™) were infected with an m.o.i. of 5–10 PFU/ml with the parental and recombinant viruses and incubated for 1 h and 24 h for each CHO cell type and frozen at −70 °C. Virus titres were determined in BHK-21 cells and viral growth was calculated by subtracting the 1 h titre results from the 24 h titre results. Positive titres were interpreted as an indication that the viruses were able to infect and replicate in the CHO cells.

2.7. Stability of vSAT1tc and SAR/9/81wt strains

The wild-type and recombinant SAT1 virus particles were concentrated with PEG (8%) and purified on 15–45% (w/v) sucrose density gradients, prepared in TNE buffer (50 mM Tris pH 7.4, 10 mM EDTA, 150 mM NaCl) as described by Knipe et al. (1997). Peak fractions corresponding to the 146S virus particles were pooled and stored at −70 °C until further use. The purified virus particles were mixed 1:50 with 2× TNE buffer ranging from pH 7.4, 7.0, 6.7, 6.3, 6.2, 6.0, 5.8 and 5.6 (±0.02) for 30 min at room temperature. Virus particles were also mixed with BME medium as control. The samples were subsequently neutralised with 1 M Tris (pH 7.4), 150 mM NaCl and titrated on BHK-21 cells or inspected with electron microscopy. The pH_{50} was determined by linear fitting of the percentage infectivity remaining following treatment at each pH point. Thermal stability of the virus particles was determined by incubating the purified particles diluted 1:50 in TNE buffer at 25, 37, 45 and 55 °C for 30 min. Following cooling on ice, the viruses were titrated on BHK-21 cells. Alternatively, the preservation and long term stability of sucrose density gradient purified virus particles were investigated using the freeze–dried method. The freeze–dried particles were treated at various temperatures of −70 °C, 4 °C, 25 °C and 37 °C for up to 42 weeks, cooled on ice, reconstituted in TNE buffer and titrated on BHK-21 cells.

2.8. Electron microscopy

Virus samples (treated with varying pH buffers or temperatures) were adsorbed to Formvar and carbon-coated nickel grids, stained with 2% (w/v) uranyl acetate for 30 s and examined in a Hitachi electron microscope operated at 80 kV. Particle sizes were determined using advanced microscopy techniques (Danvers, MA) software calibrated with grating replica (Electron Microscopy Sciences, Hatfield, PA). Images were recorded with an AMT digital camera and files were adjusted for brightness and contrast with Adobe Photoshop (Beaverton, OR).

3. Results

3.1. Accumulation of positively charge residues in the VP1 protein of SAT1/SAR/9/81 during growth in BHK-21 cells

Previously we observed that the SAT1 virus SAR/9/81tc exhibited altered plaque properties after high passage in BHK-21 cells (Maree et al., 2010). A mixture of plaque sizes (small, 1–2 mm; medium, 3–5 mm and large 7–8 mm) characterised SAR/9/81tc, while SAR/9/81wt (recovered from impala) yielded only large plaques (7–8 mm diameter) (Fig. 1A). One-step growth studies of SAR/9/81wt and SAR/9/81tc viruses in BHK-21 cells (Fig. 1B) showed that the viruses reached high titres and their growth were indistinguishable within 16 h p.i. To investigate the variation in plaque sizes in more detail we analyzed the complete genomes of SAR/9/81wt and SAR/9/81tc. Thirteen nucleotide changes were detected in the majority population of SAR/9/81tc compared to SAR/9/81wt. Of the thirteen nucleotide changes, ten resulted in amino acid changes. The six amino acid substitutions in the non-structural protein-coding regions were hypothesised to be unlikely to influence viral properties like receptor preference and cell entry, adaptation in cell culture and virion stability. However, the four amino acid differences in the capsid proteins are located in loops connecting β-sheets of the virion, one in VP3 and three in VP1. The amino acids Asn110 and Gly112 in the VP1 protein of SAR/9/81wt changed to His and Arg, respectively, following passaging in BHK-21 cells. These changes are located within the short βF-βG loop, surrounding the pore at the five-fold axis of the virion (Fig. 2A, B) and resulted in a change of electrostatic charge on the virion surface (Fig. 2C, D).

The changes in VP1 were further elucidated following a dilution series of the SAR/9/81tc virus and selecting 37 single foci of infec-

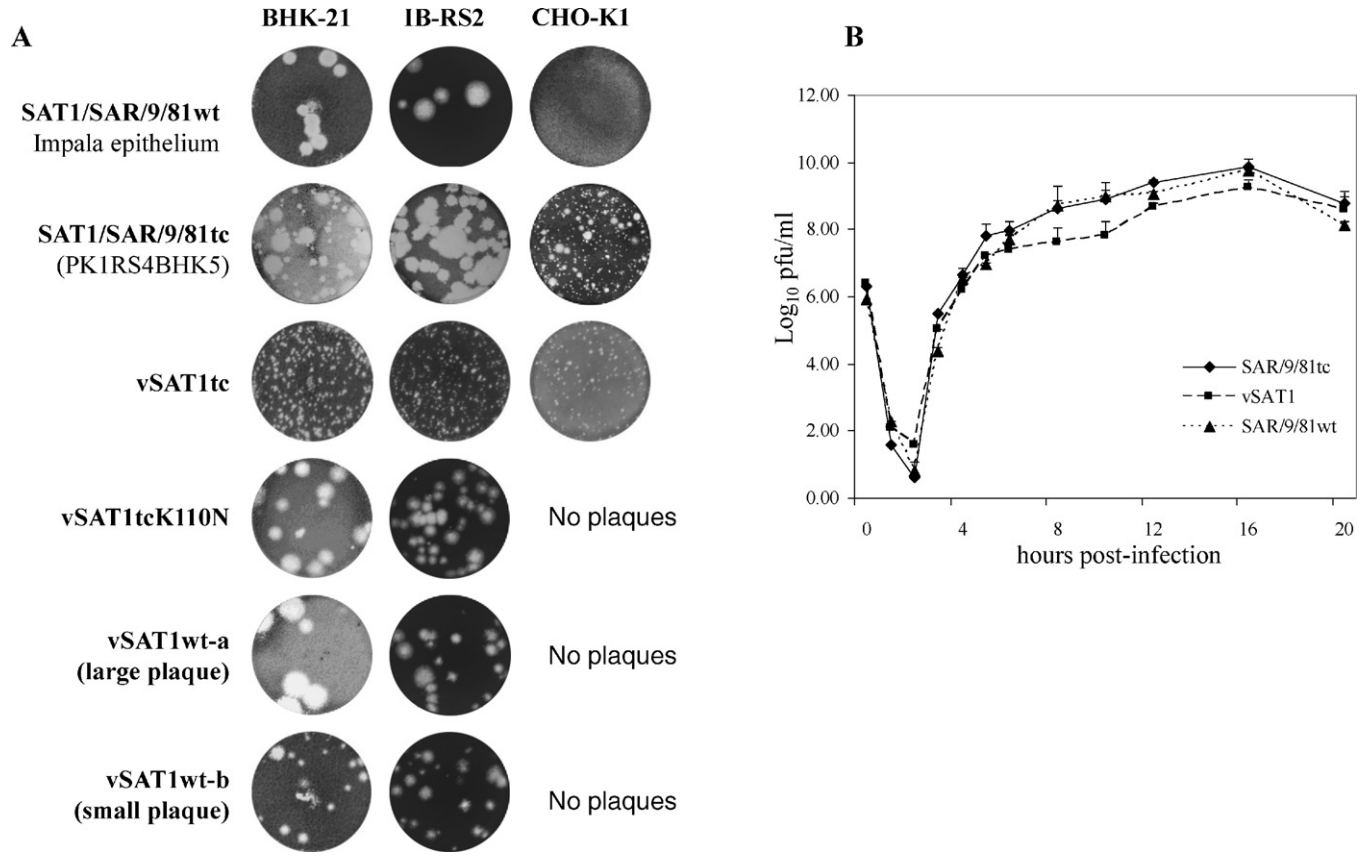

Fig. 1. (A) Plaque morphologies of the parental and genetically engineered viruses obtained using monolayers of BHK-21, IB-RS-2 and CHO-K1 cells. Cells infected with SAR/9/81tc, SAR/9/81wt, vSAT1tc, vSAT1tcK-N, vSAT1wt-a and vSAT1wt-b were incubated for either 40 h (BHK-21 and CHO-K1) or 27 h (IB-RS-2) prior to staining with methylene blue. (B) One-step growth kinetics were performed in BHK-21 cells. The average log virus titres are shown at different times p.i. with the SAR/9/81wt, SAR/9/81tc and vSAT1tc. The standard deviations of the titres determined from quadruple wells are indicated in each case. Cell monolayers were infected for 1 h at 37 °C at an m.o.i. of 2–4 PFU/ml, washed with MBS buffer (25 mM morpholine-ethanesulfonic acid, 145 mM NaCl, pH 5.5), followed by the addition of BME containing 1% FCS and continued incubation at 37 °C for 40 h. The samples were frozen at −70 °C after the specific incubation times and subsequently thawed and titrated on BHK-21 cells. Error bars indicate values obtained from duplicate titrations of samples prepared form the same experiment.

tion and sequencing of the VP1-coding region of each. The deduced VP1 amino acid sequences of the recovered viruses ($n = 37$) were compared. Sixty-three of the 218 amino acid residue positions of VP1 (~29%) were variable (Fig. 3), consistent with the quasi-species nature of the FMDV genome (Domingo et al., 1992, 2005). The variation was not uniformly distributed across VP1 but was focussed in hyper-variable regions of VP1, particularly in beta-sheet structures with hydrophilic profiles, which correlate with surface-exposed loops in the virion (data not shown). One of these regions was the βF-βG loop containing residues 110–112 that showed variations of (H/K/N)-R-(R/G) (Table 1 and Fig. 3). When the altered amino acid at position 110 was His, an Arg residue occupied position 112 in 80% of the virus population. However, when Lys was present at position 110, in 100% of the cases, Gly occupied position 112 (Table 1). In two instances the wild-type N-R-G sequence was visible. The nature of these substitutions, which resulted in an increase in positive charge

Table 1
Comparison of the deduced amino acid sequences in SAR/9/81wt, SAR/9/81tc and recombinant SAT1 viruses and the *in vitro* properties of these viruses.

FMDV strain[a]	Host/origin	Residues in protein[b]					Titre in BHK-21 cells[c]
		VP3		VP1			
		192	217	69	84	110–112	
Secondary structure		βH-βI loop	C-terminus	αA	αB	βF-βG loop	
SAR/9/81wt	Impala	Asp	Ser	Ala	Glu	Asn-Arg-Gly	5.8×10^9
SAR/9/81tc	Cell culture adapted	Tyr	Ser	Ala	Gly	(His/Lys/Asn)-Arg-(Arg/Gly)	7.2×10^9
vSAT1tc	Plasmid pSAT1tc	Tyr	Ile	Gly	Glu	Lys-Arg-Gly	4.8×10^8
vSAT1wt-a	Plasmid pSAT1wt-a	Asp	Ser	Ala	Glu	Asn-Arg-Gly	1.3×10^9
vSAT1wt-b	Plasmid pSAT1wt-b	Asp	Ser	Ala	Glu	Asn-Arg-Gly	8.6×10^8
vSAT1tc/wt	Plasmid pSAT1tc/wt	Asp	Ser	Ala	Glu	Asn-Arg-Gly	nd
vSAT1tcK-N	Plasmid pSAT1tcK-N	Tyr	Ile	Gly	Glu	Asn-Arg-Gly	9.6×10^8

[a] The abbreviation "wt" refers to the wild-type impala epithelium isolate and "tc" to the cell culture adapted version of the same isolate. The plasmid pSAT1tc was constructed from SAR/9/81tc and pSAT1wt from SAR/9/81wt. The pSAT1tc/wt was generated by replacing the outer capsid-coding region of pSAT1tc with the corresponding region of pSAT1wt. Site-directed mutagenesis of VP1 Lys110 in pSAT1tc to Asn created pSAT1tcK-N.

[b] The amino acid differences within the 1B/C/D-2A region of recombinant and the parental viruses are summarised by protein. Residue changes are indicated in italics.

[c] Titres were determined following 5 recovery passages in BHK-21 cells for vSAT1tc, vSAT1wt-a and -b, vSAT1tc/wt and vSAT1tcK-N and 5 passages of SAR/9/81wt to generate SAR/9/81tc. These virus stocks were used to study virus growth kinetics (Fig. 3A). Titres are expressed in PFU/ml.

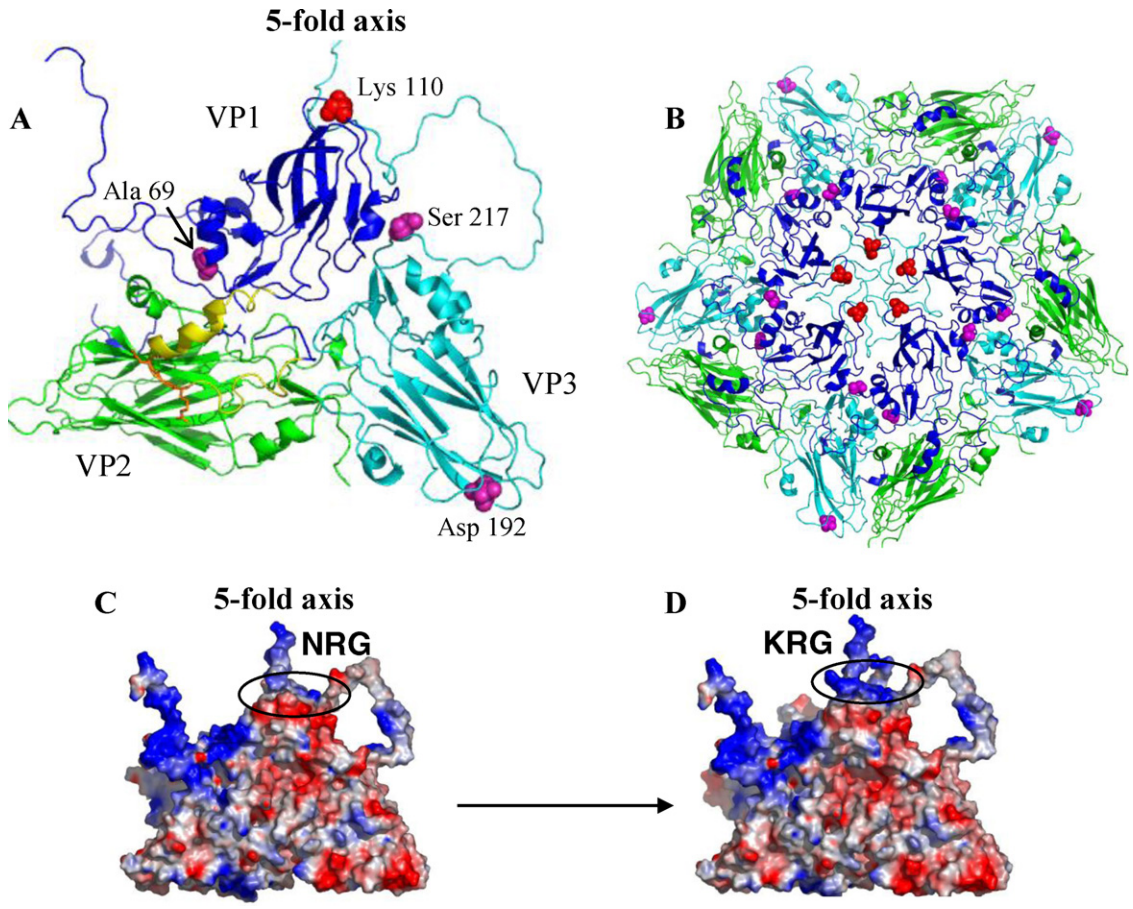

Fig. 2. 3D structure of SAR/9/81wt capsid crystallographic protomer (A) and pentamer (B) modelled using the O1BFS co-ordinates (1FOD; Logan et al., 1993) as template. The position of amino acid changes in vSAT1tc compared to the parental SAR/9/81wt is indicated. The protein subunits and structural features are colour coded: VP1 (blue), VP2 (green) and VP3 (cyan), the G–H loop of VP1 (yellow) and the RGD motif (orange). The N110K residue change is indicated in red near the five-fold axis and the remaining 3 amino acid changes in magenta. (C, D) The surface electrostatic view of protomers, containing the wild-type Asn110 at VP1 (C) and the positively charged Lys110 of vSAT1tc (D), respectively. The increased positive charge, indicated in blue, surrounds the five-fold axis of the virion.

in the local region of the five-fold axis of the virion (Fig. 2C, D), suggested that the adapted virus might attach to negatively charged cell surface structures, in particular GAG's.

3.2. Synthesis of SAT1 recombinant viruses with altered surface charges

To study the effect of the mutations at residue positions 110–112 of VP1 in a defined genetic background, we constructed infectious cDNA clones of the SAR/9/81tc and wt viruses using the infectious cDNA clone, pSAT2 (Van Rensburg et al., 2004), as template. We selected the following three infectious cDNA clones for the generation of recombinant viruses: (1) a variant of the SAR/9/81tc genome containing an Asn110 → Lys change in VP1, adding a positive charge by a single mutation, and designated pSAT1tc; (2) a genome-length clone of SAR/9/81wt containing the wild-type N-R-G sequence at residue positions 110-112 of VP1 (pSAT1wt-a); and (3) a second SAR/9/81wt genome-length clone with the wild-type N-R-G sequence, but containing an additional amino acid change in VP1, *i.e.* Ser03 → Phe (pSAT1wt-b). pSAT1tc was further characterised and found to contain four amino acid differences in the capsid sequence compared to the SAR/9/81wt virus, *i.e.* VP3 Asp192 → Tyr; VP3 Ser217 → Ile; VP1 Ala69 → Gly and VP1 Asn110 → Lys. As shown in Table 1, virus titres of the recombinant and parental viruses were similar and heterogeneity in amino acid residues was observed in only four positions in VP3 and VP1 mentioned above.

To determine the conformational location of these substitutions in the capsid, the changes were mapped to the 3D structure of the SAR/9/81 capsid. As illustrated in Fig. 2A and B, two of the substitutions (Asp192 → Tyr, and Ser217 → Ile) are located on flexible loops connecting the β-sheet structures of VP3, while the Ala69 → Gly change in VP1 is found in an α-helix hidden from the surface. The Ala69 → Gly change is also distant from the βG-βH loop of VP1 that contains the receptor-binding RGD motif, and all three changes are distantly located to the sites known to participate in HSPG binding of type O viruses (Fry et al., 1999, 2005; Sa-Carvalho et al., 1997; Zhao et al., 2003). In contrast, the Asn110 → Lys change not only adds a positive charge to the surface of the viral capsid, but also clusters around the pore at the five-fold axis of the particle (Fig. 2). The presence of Lys110 in pSAT1 is consistent with the His/Lys quasi-species observed in the SAR/9/81tc, but not the SAR/9/81wt virus (Table 1 and Fig. 3).

Based on the structural analysis, we performed the following mutations or genome exchanges in the infectious clones: (1) The Lys residue at position 110 of VP1 in the pSAT1tc clone was mutated to the wild-type Asn residue (pSAT1tcK-N); and (2) the outer capsid-coding region of pSAT1tc was replaced with the corresponding region of pSAT1wt-a (pSAT1tc/wt).

The corresponding recombinant and mutant viruses, designated vSAT1tc, vSAT1wt-a, vSAT1wt-b, vSAT1tcK-N and the vSAT1tc/wt chimera, were recovered following the co-transfection of the recombinant plasmids and a helper plasmid into BHK-21 cells. The genetic identities of the recovered virus stocks were confirmed by

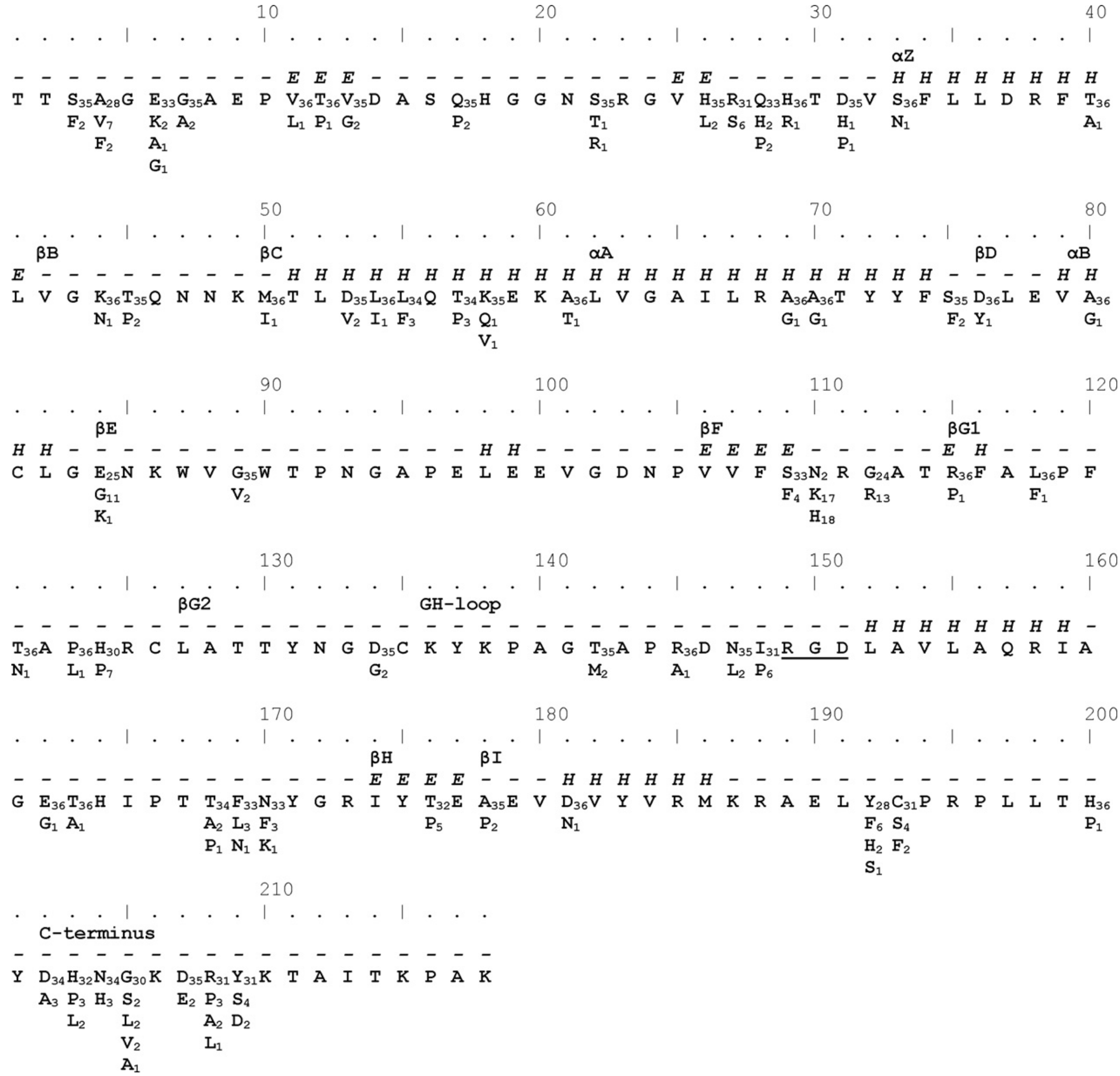

Fig. 3. Amino acid variability of the VP1 protein of SAR/9/81tc is shown next to the consensus sequence of the virus population. The subscript number next to the residue indicates the number of times that particular residue was observed. Regions corresponding to beta sheets are indicated by an "E" above the consensus sequence, regions corresponding to alpha helices are shown as "H" and the RGD motif within the βG-βH loop are underlined.

nucleotide sequencing of the capsid-coding region and no unintentional mutations were observed. The r1-values obtained for vSAT1tc (Table 2) with sera raised against SAR/9/81, the genetically related SAT1/KNP/196/91 virus and the disparate SAT1/NIG/5/81 virus, revealed no antigenic differences between the recombinant vSAT1tc and the parental SAR/9/81tc or SAR/9/81wt viruses. The Lys at position 110 did not seem to alter the antigenicity of vSAT1tc based on r1-values.

3.3. In vitro characterisation of genetically engineered FMDVs

The effect of these mutations on viral growth in BHK-21 cells was investigated. The genetically engineered vSAT1tc displayed small plaques (1–2 mm diameter) equivalent to those of SAR/9/81tc virus from which it was generated (Fig. 1A). The two variants from the wild-type infectious clones, vSAT1wt-a and vSAT1wt-b, produced large (6–8 mm) and medium plaques (3–5 mm) with opaque edges, respectively. The medium plaques of vSAT1wt-b also differed from the small plaques produced by pSAT1tc in that the latter were well-defined morphology. A porcine kidney cell line (IB-RS-2) known to express $\alpha_V\beta8$ (Burman et al., 2006), was also included in the analysis. Although the plaques were generally larger on IB-RS-2 cells after 40 h incubation (data not shown), a shorter incubation time (27 h) showed the distribution of large and small plaques were similar to those described on BHK-21 cells (Fig. 1A). In CHO-K1 cells, only cell culture-adapted SAR/9/81tc and vSAT1tc viruses were able to propagate. The micro-size plaques (<2 mm) produced in CHO-K1 cells were only visible 48 h post-infection (p.i.) (Fig. 1A).

Plaque assays performed on BHK-21 cells revealed large plaques (6 mm) for the vSAT1tcK-N mutant. The plaques corresponded in size and character with plaques produced by SAR/9/81wt, vSAT1wt-a (Fig. 1A) and vSAT1tc/wt (data not shown). The vSAT1tcK-N mutant was unable to infect CHO-K1 cells, similar to the wild-type viruses (Fig. 1A). The conversion of small plaques to wild-type plaques by the Lys110 → Asn mutation is a clear indication that the BHK-21 adaptation phenotype is a charge-based interaction, perhaps involving binding to cell surface sulphated polysaccharides.

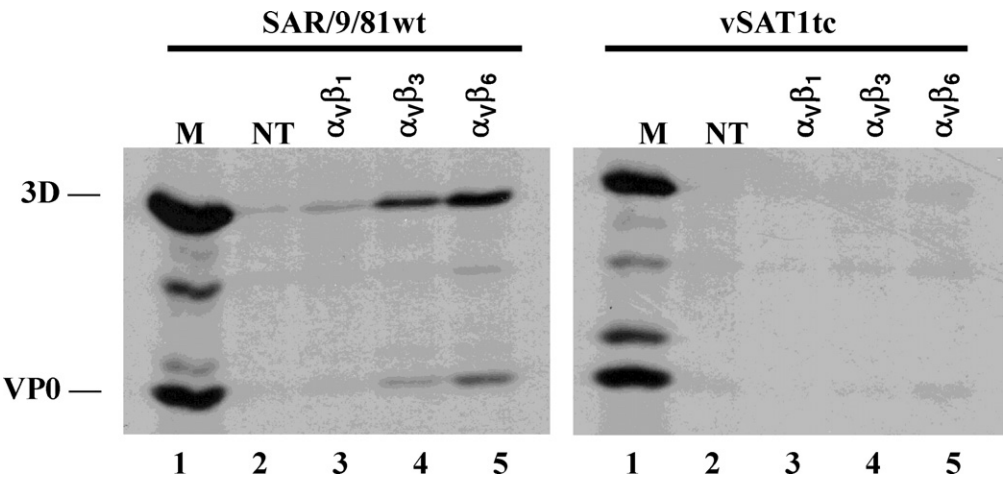

Fig. 4. COS-1 cells were co-transfected with cDNA plasmids encoding the bovine integrin α_V subunit and either the β1, β3 or β6 subunits (Neff and Baxt, 2001). Transfected cells were infected with SAR/9/81wt or vSAT1tc and proteins were radiolabelled with [^{35}S]methionine. Viral protein syntheses were analyzed by RIP and SDS-PAGE. Immunoprecipitated proteins from nontransfected-infected cell-lysates are indicated by "NT", and the location of the viral structural proteins from lysates prepared from FMDV-infected BHK-21 cells is indicated by "M".

The infectivity titres after an endpoint dilution revealed that the titre of the SAR/9/81tc virus (7.2×10^9) was higher than vSAT1tc (4.8×10^8) in BHK-21 cells (Table 1). The titres of SAR/9/81wt (5.8×10^9) and vSAT1wt-a (1.3×10^9) appeared similar to that of SAR/9/81tc, while the titres of vSAT1wt-b and vSAT1tcK-N mutant were 8.6×10^8 and 9.6×10^8 in BHK-21 cells (Table 1). The growth kinetics of the vSAT1tc (Fig. 1B) in BHK-21 cells show that vSAT1tc reached similar high virus titres within 16 and 20 h p.i. than SAR/9/81tc and SAR/9/81wt.

3.4. Binding of the SAT1 viruses to cells in culture

The receptor specificity of the SAR/9/81wt, SAR/9/81tc and vSAT1tc viruses was investigated. To this end, two types of CHO cells, *i.e.* CHO-K1 and CHO-677 were infected using high multiplicity of infection (m.o.i. 1–5 pfu/cell) with the respective SAT1 viruses. The SAR/9/81wt viruses were not able to replicate in these CHO cell types. However, a titre of 1.1×10^6 pfu/ml was attained from vSAT1tc-infected CHO-K1 cells. Similarly, SAR/9/81tc grew to a titre of 2×10^6 pfu/ml in CHO-K1 cells. Since neither of these viruses was able to infect and replicate in CHO-677 cells, cell entry was most probably initiated by attachment to GAG surface molecules. None of the recombinant viruses or vSAT1tcK-N mutant virus containing the wild-type VP1 sequence was able to replicate in CHO-K1 cells.

The integrin receptor specificity of these viruses was explored in COS-1 cells, co-transfected with bovine α_V integrin subunit and either of the β1, β3 or β6 subunit cDNAs. Replication of the SAR/9/81wt virus was demonstrated in cultured cells expressing $\alpha_V\beta6$ (Fig. 4). The bovine $\alpha_V\beta3$ integrin was also utilised for cell entry by this impala isolate of SAT1, albeit to a lesser extent. The bovine αvβ1 was not able to sustain infection for any of these viruses. Although the interaction with $\alpha_v\beta8$ intergrins was not measured directly, IB-RS2 cells, known to have this integrin predominantly on its cell surface (Burman et al., 2006) were able to sustain infection of SAR/9/81wt to high titres.

Given that SAR/9/81wt virus displayed the ability to recognise and enter cells expressing bovine $\alpha_V\beta6$ and $\alpha_V\beta3$, it was surprising to find that vSAT1tc replicated poorly in cells expressing these bovine integrins (Fig. 4). In contrast, this variant infected and replicated in CHO-K1 cells, but not CHO-677 cells, suggesting the use of alternative HSPG cell surface proteins. The acquisition of positively charged Asn110 → Lys (one of the four amino acid differences detected in vSAT1tc), surrounding the five-fold axis, could potentially account for interaction with negatively charged cell surface molecules, like GAGs.

Table 2
Comparison of the antigenicity of SAT1 parental and recombinant viruses measured against SAT1 reference sera.

Viruses	r1-value[a]			
	SAT1 test sera[b]			
	KNP/196/91[c]	SAR/9/81	KNP&SAR	NIG/5/81[d]
SAT1				
KNP/196/91	**1.00**	0.40 ± 0.14	**1.00**	0.17 ± 0.03
SAR/9/81tc	0.45 ± 0.06	**1.00**	**1.00**	0.25 ± 0.06
SAR/9/81wt	0.40 ± 0.05	**1.00**	**1.00**	0.24 ± 0.06
vSAT1tc	0.38 ± 0.03	**1.00**	**1.00**	0.18 ± 0.04

[a] VNTs were done in duplicate. r1-values are expressed as the ratio between the heterologous/homologous end point serum titres of the largest dilution of serum to neutralise 100 $TCID_{50}$ in 50% of the wells in VN tests. The homologous r1-values are indicated in bold.
[b] The cattle sera used in the VN tests were prepared by two consecutive vaccinations on days 0 and 28 with reference SAT1 or SAT2 viruses and subsequently bled on day 38.
[c] The SAT1/KNP/196/91 virus, isolated in 1996 from buffalo in the Kruger National Park, and homologous serum prepared by vaccinating cattle was included as a SAT1 control in the VN assay.
[d] The SAT1/NIG/5/81 virus, isolated in 1981 from Nigeria, belongs to the SAT1 topotype 7 lineage (Bastos et al., 2001).

3.5. Assessment of vSAT1tc and SAR/9/81wt virus particle stability

During sucrose density gradient (SDG) purification of vSAT1tc virus (which had acquired positively charged residues), we noticed a small 146S peak determined at 260 nm that contrasted to the SAR/9/81wt clear virus peak. Furthermore, by increasing the salt concentration from 150 to 500 mM NaCl, a defined 146S peak for the vSAT1tc variant particles was observed (data not shown) suggesting that the additional positive charges may enhance aggregation of the vSAT1tc virus particles. In addition the sensitivity of the infectious particles in an acidic environment was evaluated. The pH-stability profiles in Fig. 5A show a slight difference in particle stability when vSAT1tc and SAR/9/81wt viruses were incubated in mild acidic conditions that was not statistically significant over the entire pH range ($P = 0.437$). However, there was a significant difference in particle stability for pH ≤ 6.2 ($P = 0.050$). In particular, a $pH_{50} = 6.45$ value was obtained for SAR/9/81wt, while a $pH_{50} = 6.35$ distinguished the vSAT1tc variant. Based on

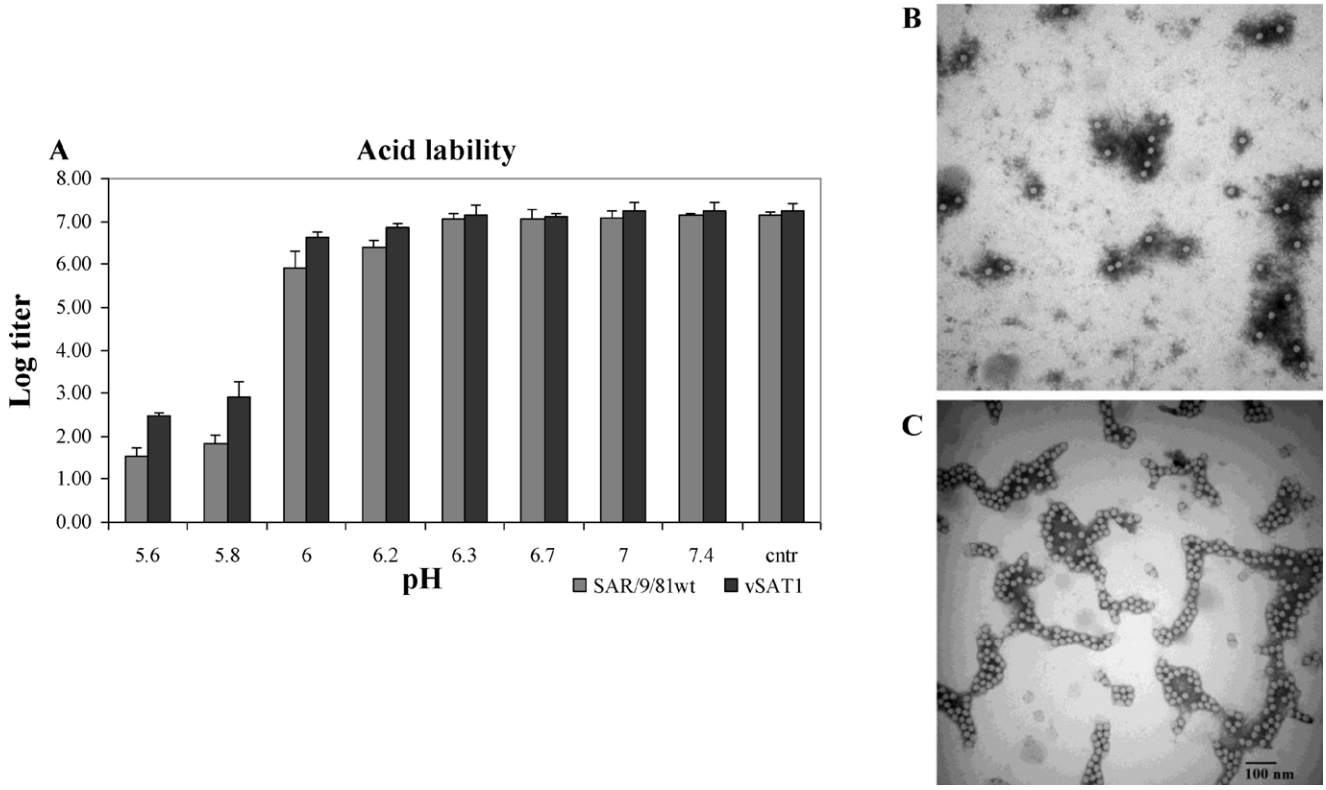

Fig. 5. pH inactivation kinetics of SAR/9/81wt and vSAT1tc viruses. (A) Inactivation of SDG-purified wild-type and vSAT1tc particles following treatment with TNE (100 mM Tris, 150 mM NaCl, 10 mM EDTA) buffers ranging from pH 7.4 to 5.6 for 30 min. The average virus titres of two inactivation experiments at each pH are plotted. (B, C) SDG-purified SAR/9/81wt (B) and vSAT1tc (C) viruses, treated with TNE buffers of varying pH, were adsorbed on Formvar and carbon-coated grids. Samples were negatively stained with 2% uranyl acetate (UA), pH 7.4, imaged and viewed at 100,000× magnification. The vSAT1tc showed extensive aggregation at pH 6.5, even after vigorous vortexing.

the nature (Table 1) and location (Fig. 2A, B) of the amino acid differences between vSAT1tc and SAR/9/81wt capsid proteins, it was hypothesised that Asp192 → Tyr, Ser217 → Ile in VP3 and Asn110 → Lys in VP1 could account for the differences in stability observed over the lower pH values. Electron microscopic studies (Fig. 5C) showed the presence of aggregates for the vSAT1tc virus even at pH 6.5, but not for the SAR/9/81wt (Fig. 5B). The aggregates of vSAT1tc have been observed from pH 7.4 (data not shown) to pH 6.5 and could possibly account for the difficulties encountered during purification of the vSAT1tc variant (see above).

Incubation of the infectious particles between 25 °C and 45 °C for 30 min resulted in an equivalent decrease in infectivity with less than 2% of infectious particles remaining after 30 min treatment at 45 °C (results not shown). The stability of purified, lyophilised SAR/9/81wt and vSAT1tc viruses was further investigated by long-term storage at −70 °C, 4 °C, 25 °C and 37 °C. For reasons not well understood there was a significant loss of infectious particles (ca. 33 ± 6.5% loss) within the first day in all instances (Fig. 6). However, thereafter the titres remained constant for up to 16 weeks at 4 °C or 25 °C with more variable values at 37 °C. At 52 weeks incubation at 25 °C and 37 °C no infectivity titres could be detected, while 2 logs reduction was measured at 4 °C for vSAT1tc and SAR/9/81wt (Fig. 6). Overall, no significant differences were observed between the two viruses under these experimental conditions, and as expected, storage at −70 °C (Fig. 6A) was the most effective method to preserve FMDV infectivity for extended periods of time.

4. Discussion

In spite of virus–integrin interaction being essential for infectivity of FMDV in cattle, or *in vitro* in cell culture, propagation of FMDV in non-host cells, like BHK-21 cells, leads to rapid change in the preference of cell surface molecules used for cell entry (Jackson et al., 1996; Baranowski et al., 1998). In this study we describe the fixation of amino acid residues during the propagation of a SAT1 virus obtained from impala in BHK-21 cells. An infectious SAT1 genome-length clone, vSAT1tc, from the quasi-species population of a SAT1 cell culture-adapted virus displayed a small plaque phenotypic variant of the initial mixed plaque size of the SAR/9/81tc population. The vSAT1tc did not have a perfect nucleotide and amino acid match to the majority population of SAR/9/81tc from which it was derived, an observation consistent with the quasi-species nature of the FMDV genome (Domingo et al., 1992, 2005; Domingo, 1998). The four amino acid differences in the outer capsid-coding region of the pSAT1tc clone (Table 1) were also present in single foci of SAR/9/81tc.

The fixation of the positively charged residues, Lys110 and Arg111, in the short βF-βG loop 110KRG112 sequence surrounding the five-fold axis of the SAR/9/81tc and vSAT1tc virions relates to the acquisition of the ability to replicate in CHO-K1 cells, but not CHO-677 cells, and a small plaque size on BHK-21 cells. The *in vitro* observations for the viruses in this study, suggest possible interaction with negatively charged GAGs, which are abundant cell surface proteins that has been linked to cell attachment of FMDV adapted to cultured BHK-21 cell (Gromm et al., 1995; Jackson et al., 1996; Sa-Carvalho et al., 1997). Mutation of the Lys110 of vSAT1tc to the wild-type Asn resulted in the conversion of small plaques to large plaques on BHK-21 cells and abrogated the ability to infect CHO-K1 cells, indications of the role of VP1 residues 110 and 111 in cell culture adaptation and possible interaction with GAGs. The VP1 βF-βG loop in the capsid has been shown in a comparison of 56 SAT1 and SAT2 viruses to be hypervariable, while none of the viruses in this alignment displayed a significant positively charged

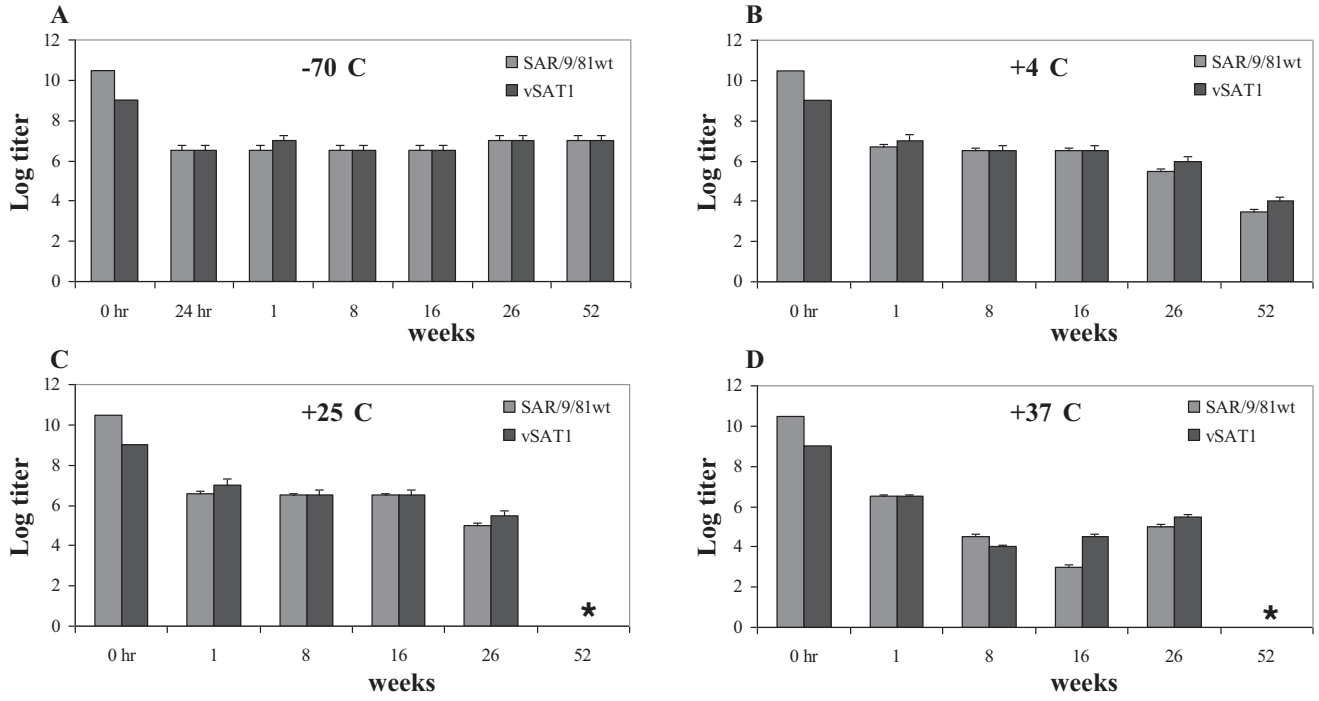

Fig. 6. Thermal inactivation kinetics of SAR/9/81wt and recombinant vSAT1tc viruses. SDG-purified virus was lyophilised, incubated at (A) −70 °C, (B) 4 °C, (C) 25 °C and (D) 37 °C and the log virus titre plotted against 0 or 24 h and up to 52 weeks of incubation. (*) Error bars indicate values obtained from duplicate titrations of samples prepared form the same experiment. No infectious particles were observed at 52 weeks incubation at 25 °C and 37 °C.

region at this position (Maree et al., 2010) and is unlikely to exhibit the ability to infect and replicate in CHO-K1 cells, like SAR/9/81wt (Fig. 4A) and SAT1/NAM/307/98 (Storey et al., 2007).

An in-depth look at the residues present in the VP1 βF-βG loop in the SAR/9/81tc population revealed that if an Asn, His or Lys residue is fixated at amino acid 110, an Arg, Lys or Gly is acquired at position 112 in the adapted strain. The Arg111 in the 110NRG112 sequence, in the absence of other positively charged residues, was not sufficient to enable SAR/9/81wt to infect CHO-K1 cells. The amino acid variation at positions 110–112 in VP1 also correlates with the mixed plaque phenotypes that were observed.

Notwithstanding the differences in the plaque morphologies amongst SAR/9/81wt, SAR/9/81tc, and the vSAT1tc derivative, optimal growth kinetics in BHK-21 cells were maintained in vSAT1tc, a characteristic desired for a suitable vaccine candidate. Likewise, the antigenicity of the SAR/9/81 (wt and tc) viruses seemed to be unchanged in vSAT1tc based on limited cross neutralization data. Overall the data indicated that the replication machinery as well as antigenic and biological properties of the parental virus were successfully transferred to the recombinant vSAT1tc.

The increase in positive charge in the local region on the virion surface suggests that the adaptation phenotype possibly involves interaction with cell surface sulphated polysaccharides, like GAG. It has been proposed that virus uptake might be accelerated via direct interactions between HSPG's and integrin receptors, since other adhesion molecules, like vitronectin and fibronectin also have dual affinity for integrin and heparin sulphate (Gromm et al., 1995; Fry et al., 1999, 2005). Therefore, the possibility that BHK-21 culture-adapted viruses that acquire HSPG-binding ability are dependent on the dual affinity for both HSPG and integrin proteins to enter and infect cells, cannot be excluded.

Earlier studies on FMDV receptor preference focussed mainly on the Euro-Asian (A and O) FMDV types isolated from domestic animals (Berinstein et al., 1995; Neff et al., 1998,2000; Neff & Baxt, 2001; Jackson et al., 1997, 2000, 2002, 2004; Duque & Baxt, 2003; Monaghan et al., 2005). Here we provided the first evidence that a SAT1 virus, isolated from infected impala and with the ability to infect multiple wildlife and domestic species, utilise the $\alpha_V\beta6$ integrin with high efficiency, followed by the ability to interact with $\alpha_V\beta3$, albeit to a lesser extent. Contrary to the situation with type O_1 viruses that utilise $\alpha_V\beta1$ and $\alpha_V\beta6$ with high efficiency (Jackson et al., 2002; Duque & Baxt, 2003), the $\alpha_V\beta1$ integrins were not able to sustain infection of the SAT1 viruses.

The relevance of the virion stability in the production of stable 146S antigen and the practical aspect of vaccine efficacy are important considerations for vaccine manufacturers. A parallel comparison of the pH stability of SAR/9/81wt and vSAT1tc indicated a statistical significant difference in the particle stability of these viruses at the lower pH range. Predictions based on the structural data do not suggest that the observed amino acid heterogeneity within VP3 (Asp192 → Tyr and Ser217 → Ile) of SAR/9/81wt and vSAT1tc affect virion stability adversely. Similarly, the Ala69 → Gly change in VP1 has no effect on the polarity at that position. Hydrogen bond analysis showed that hydrogen bonds with the backbone of the intra-chain Ile64 was conserved (data not shown) and is not expected to interfere in the interaction of adjacent protomers.

The aggregation observed during SDG purification of vSAT1tc can be reversed by increasing the ionic strength of the buffer solution. This led us to formulate two hypotheses: (1) The sulphated polysaccharides interact with the particles and result in aggregates consisting of particles linked by the free polyanions and/or (2) The positively charged local regions on the capsid form electrostatic interactions with negatively charged patches on the shell of adjacent particles. Treatment with 0.5 M NaCl, Tris buffers resulted in the dissociation of these aggregates and purification of a well-defined 146S peak containing complete infectious particles. Surface coverage of the virion with the polyanions due to the positively charged Lys110 and the Arg111 residues and the aggregation of particles may have a stabilising effect in adverse environmental conditions. Evaluation of the SAR/9/8wt and vSAT1tc revealed that storage of vacuum-dried purified, life virus particles provided an

effective method to preserve infectivity. This method of preservation also allowed efficient storage at a wide range of temperatures, including −70 °C to 25 °C.

BHK-21 cells are the cell line of choice for production of inactivated FMD vaccines. The adaptation of SAT field viruses to BHK-21 cells is essential to produce high yields of 146S antigen. The addition of the cell culture-adaptation trait with the slight improvement of virion stability, using a reverse genetic approach, may improve yield of inactivated antigen during production. Furthermore, the positively charged amino acid accumulated during BHK-21 culture adaptation does not appear to adversely affect antigenicity, based on limited cross neutralization data, or thermostability of the purified SAT1 particles. In conclusion, we presented evidence for the design and improvement of genetic engineered viruses to be used as cell-adapted vaccine candidates for mitigation of FMD outbreaks.

Acknowledgements

This work was supported by funding from Intervet and the U.S. Department of Agriculture, Agricultural Research Service.

Many thanks to Michael LaRocco for providing the COS cells, expressing the integrins utilised in this study. We thank Ed Kramer for his contributions with virus titrations, Tjaart de Beer who provided the modelled structures and Geoff Fosgate for statistical analysis. We would also like to thank Dr. B. Baxt for many fruitful discussions and Ms. Sonja Maree and Erika Kirkbride for critical reading of the manuscript.

References

Amadori, M., Berneri, C., Archetti, I.L., 1994. Immunogenicity of foot-and-mouth disease virus grown in BHK-21 suspension cells. Correlation with cell ploidy alterations and abnormal expression of the alpha 5 beta 1 integrin. Vaccine 12, 159–166.

Amadori, M., Volpe, G., Defilippi, P., Berneri, C., 1997. Phenotypic features of BHK-21 cells used for production of foot-and-mouth disease vaccine. Biologicals 25, 65–73.

Bachrach, H.L., 1968. Foot-and-mouth disease. Annu. Rev. Microbiol. 22, 201–244.

Baranowski, E., Sevilla, N., Verdaguer, N., Ruiz-Jarabo, C.M., Beck, E., Domingo, E., 1998. Multiple virulence determinants of foot-and-mouth disease virus in cell culture. J. Virol. 72 (8), 6362–6372.

Bastos, A.D.S., Bertschinger, H.J., Cordel, C., Van Vuuren, C.de W.J., Bengis, R.G., Grobler, D.G., Thomson, G.R., 1999. Possibility of sexual transmission of foot-and-mouth disease from African buffalo to cattle. Vet. Rec. 17, 77–79.

Bastos, A.D.S., Haydon, D.T., Forsberg, R., Knowles, N.J., Anderson, E.C., Nel, L.H., Thomson, G.R., Bengis, R.G., 2001. Genetic heterogeneity of SAT-1 type foot-an-d-mouth disease viruses in southern Africa. Arch. Virol. 146, 1537–1551.

Bastos, A.D.S., Haydon, D.T., Sangare, O., Boshoff, C.I., Edrich, J.L., Thomson, G.R., 2003a. The implications of virus diversity within the SAT 2 serotype for control of foot-and-mouth disease in sub-Saharan Africa. J. Gen. Virol. 84, 1595–1606.

Bastos, A.D.S., Anderson, E.C., Bengis, R.G., Keet, D.F., Winterbach, H.K., Thomson, G.R., 2003b. Molecular epidemiology of SAT3-type foot-and-mouth disease. Virus Genes 27, 283–290.

Baxt, B., Becker, Y., 1990. The effect of peptides containing the arginine–glycine–aspartic acid sequence on the adsorption of foot-and-mouth disease virus to tissue culture cells. Virus Genes 4, 73–83.

Berinstein, A., Roivainen, M., Hovi, T., Mason, P.W., Baxt, B., 1995. Antibodies to the victronectin receptor integrin $\alpha_v\beta3$ inhibit binding and infection of foot-and-mouth disease virus to cultured cells. J. Virol. 69, 2664–2666.

Burman, A., Clark, S., Abrescia, N.G., Fry, E.E., Stuart, D.I., Jackson, T., 2006. Specificity of the VP1 GH loop of foot-and-mouth disease virus for α_v integrins. J. Virol. 80, 9798–9810.

Dawe, P.S., Flanagan, F.O., Madekurozwa, R.L., Sorensen, K.J., Anderson, E.C., Foggin, C.M., Ferris, N.P., Knowles, N.J., 1994. Natural transmission of foot-and-mouth disease virus from African buffalo (Syncerus caffer) to cattle in a wildlife area of Zimbabwe. Vet. Rec. 134, 230–232.

Domingo, E., Escarmis, C., Martinez, M.A., Martinez-Salas, E., Mateu, M.G., 1992. Foot-and-mouth disease virus populations are quasispecies. Curr. Top. Microbiol. Immunol. 176, 33–47.

Domingo, E., 1998. Quasispecies and the implications for virus persistence and escape. Clin. Diagn. Virol. 10, 97–101.

Domingo, E., Escarmis, C., Lázaro, E., Manrubia, S.C., 2005. Quasispecies dynamics and RNA virus extinction. Virus Res. 107, 129–139.

Duque, H., Baxt, B., 2003. FMDV receptors: comparison of bovine α_v integrin utilization by type A and O viruses. J. Virol. 77, 2500–2511.

Duque, H., LaRocco, M., Golde, W.T., Baxt, B., 2004. Interactions of foot-and-mouth disease virus with soluble bovine alphaVbeta3 and alphaVbeta6 integrins. J. Virol. 78 (18), 9773–9781.

Esterhuysen, J.J., Thomson, G.R., Ashford, W.A., Lentz, D.W., Gainaru, M.D., Sayer, A.J., Meredith, C.D., Janse van Rensburg, D., Pini, A., 1988. The suitability of a rolled BHK21 monolayer system for the production of vaccines against the SAT types of foot-and-mouth disease virus. I. Adaptation of virus isolates to the system, immunogen yields achieved and assessment of subtype cross reactivity. Onderstepoort. J. Vet. Res. 55 (2), 77–84.

Fox, G., Parry, N.R., Barnett, P.V., McGinn, B., Rowlands, D.J., Brown, F., 1989. The cell attachment site on foot-and-mouth disease virus includes the amino acid sequence RGD (arginine–glycine–aspartic acid). J. Gen. Virol. 70 (Pt. 3), 625–637.

Fry, E.E., Lea, S.M., Jackson, T., Newman, J.W.I., Ellard, F.M., Blakemore, W.E., Abu-Ghazaleh, R., Samuel, A., King, A.M.Q., Stuart, D.I., 1999. The structure and function of a foot-and-mouth disease virus–oligosaccharide receptor complex. EMBO J. 18 (3), 543–554.

Fry, E.E., Newman, J.W.I., Curry, S., Najjam, S., Jackson, T., Blakemore, W., Lea, S.M., Miller, L., Burman, A., King, A.M.Q., Stuart, D.I., 2005. Structure of FMDV serotype $A1O_{61}$ alone and complexed with oligosaccharide receptor: receptor conservation in the face of antigenic variation. J. Gen. Virol. 86, 1909–1920.

Gromm, J.R., Hilemann, R.E., Caldwell, E.E.O., Weiler, J.M., Linhardt, R.J., 1995. Differences in the interaction of heparin with arginine and lysine and the importance of these basic amino acids in the binding of heparin to acidic fibroblast growth factor. Arch. Biochem. Biophys. 323, 279–287.

Heath, L., 2008. Information on the distribution of SAT-type foot-and-mouth disease viruses in African buffalo (*Syncerus caffer*) populations. Technical report to the Food, Agriculture and Natural Resources Directorate of the Southern African Development Community Secretariat.

Jackson, T., Ellard, F.M., Abu-Ghazaleh, R., Brookes, S.M., Blakemore, W.E., Corteyn, A.H., Stuart, D.I., Newman, J.W.I., King, A.M.Q., 1996. Efficient infection of cells in culture by type O foot-and-mouth disease virus requires binding to cell surface heparan sulfate. J. Virol. 70, 5282–5287.

Jackson, T., Sharma, A., Ghazaleh, R.A., Blakemore, W.E., Ellard, F.M., Simmons, D.L., Newman, J.W.I., Stuart, D., King, A.M.Q., 1997. Arginine–glycine–aspartic acid-specific binding by foot-and-mouth disease viruses to the purified integrin $\alpha_v\beta3$ *in vitro*. J. Virol. 71 (11), 8357–8361.

Jackson, T., Sheppard, D., Denyer, M., Blakemore, W., King, A.M.Q., 2000. The epithelial integrin alpha-v-beta-6 is a receptor for foot-and-mouth disease virus. J. Virol. 74 (11), 4949–4956.

Jackson, T., Mould, A.P., Sheppard, D., King, A.M.Q., 2002. Integrin $\alpha_v\beta1$ is a receptor for foot-and-mouth disease virus. J. Virol. 76, 935–941.

Jackson, T., Clarck, S.J., Berryman, S., Burman, A., Cambier, S., Mu, D., Nishimura, S., King, A.M.Q., 2004. Integrin a $\alpha_v\beta8$ functions as a receptor for foot-and-mouth disease virus: role of the b-chain cytodomain in integrin-mediated infection. J. Virol. 78, 4533–4540.

Knipe, T., Rieder, E., Baxt, B., Ward, G., Mason, P.W., 1997. Characterization of synthetic foot-and-mouth disease virus provirions separates acid-mediated disassembly from infectivity. J. Virol. 71, 2851–2856.

Knowles, N.J., Samuel, A.R., 2003. Molecular epidemiology of foot-and-mouth disease virus. Virus Res. 91, 65–80.

Logan, D., Abu-Ghazaleh, R., Blakemore, W., Curry, S., Jackson, T., King, A., Lea, S., Lewis, R., Newman, J., Parry, N., Rowlands, D., Stuart, D., Fry, E., 1993. Structure of a major immunogenic site on foot-and-mouth disease virus. Nature 362, 566–568.

Maree, F.F., Blignaut, B., De Beer, T.A.P., Visser, N., Rieder, E., 2010. Mapping of amino acid residues responsible for adhesion of cell culture-adapted foot-and-mouth disease SAT type viruses. Virus Res. 153, 82–91.

Mason, P.W., Rieder, E., Baxt, B., 1994. RGD sequence of foot-and-mouth disease virus is essential for infecting cells via the natural receptor but can be bypassed by an antibody-dependent enhancement pathway. Proc. Natl. Acad. Sci. U.S.A. 91, 1932–1936.

Monaghan, P., Gold, S., Simpson, J., Zhang, Z., Weinreb, P.H., Violette, S.M., Alexandersen, S., Jackson, T., 2005. The $\alpha_v\beta6$ integrin receptor for foot-and-mouth disease virus is expressed constitutively on the epithelial cells targeted in cattle. J. Gen. Virol. 86, 2769–2780.

Neff, S., Sa-Carvalho, D., Rieder, E., Mason, P.W., Blystone, S.D., Brown, E.J., Baxt, B., 1998. Foot-and-mouth disease virus virulent for cattle utilizes the integrin alpha(v)beta3 as its receptor. J. Virol. 72, 3587–3594.

Neff, S., Mason, P.W., Baxt, B., 2000. High-efficiency utilization of the bovine integrin $\alpha_v\beta3$ as a receptor for foot-and-mouth disease virus is dependent on the bovine $\beta3$ subunit. J. Virol. 74, 7298–7306.

Neff, S., Baxt, B., 2001. The ability of integrin alpha(v)beta(3) to function as a receptor for foot-and-mouth disease virus is not dependent on the presence of complete subunit cytoplasmic domains. J. Virol 75, 527–532.

Office International des Epizooties, 2009. Manual of Diagnostic Tests and Vaccines for Terrestrial Animals. Office International des Epizooties, Paris, France, Chapter 2.1.5, pp 1–25.

Pay, T.W.F., Rweyemamu, M.M., O'Reilly, K.J., 1978. Experiences with Type SAT 2 foot-and-mouth disease vaccines in Southern Africa. XVth Conference of the Office International Des Epizzoties Permanent Commision on foot-and-mouth disease. pp 1–25.

Parry, N., Fox, G., Rowlands, D., Brown, F., Fry, E., Acharya, R., Logan, D., Stuart, D., 1990. Structural and serological evidence for a novel mechanism of antigenic variation in foot-and-mouth disease virus. Nature 347, 569–572.

Pfaff, E., Thiel, H.-J., Beck, E., Strohmaier, K., Schaller, H., 1988. Analysis of neutralizing epitopes on foot-and-mouth disease virus. J. Virol. 62 (6), 2033–2040.

Preston, K.J., Owens, H., Mowat, G.N., 1982. Sources of variations encountered during the selection and production of three strains of FMD virus for the development of vaccine for use in Nigeria. J. Biol. Stand. 10, 35–45.
Rieder, E., Bunch, T., Brown, F., Mason, P.W., 1993. Genetically engineered foot-and-mouth disease viruses with poly(C) tracts of two nucleotides are virulent in mice. J. Virol. 67, 5139–5145.
Rieder, E., Henry, T., Duque, H., Baxt, B., 2005. Analysis of a foot-and-mouth disease type A_{24} isolate containing an SGD receptor recognition site in vitro and its pathogenesis in cattle. J. Virol. 79, 12989–12998.
Rweyemamu, M.M., 1978. The selection of vaccine strains of foot and mouth disease virus. Br. Vet. J. 134, 63–67.
Sa-Carvalho, D., Rieder, E., Baxt, B., Rodarte, R., Tanuri, A., Mason, P.W., 1997. Tissue culture adaptation of foot-and-mouth disease virus selects viruses that bind to heparin and are attenuated in cattle. J. Virol. 71, 5115–5123.
Storey, P., Theron, J., Maree, F.F., O'Neill, H.G., 2007. A second RGD motif in the 1D capsid protein of a SAT1 type foot-and-mouth disease virus field isolate is not essential for attachment to target cells. Virus Res. 124 (1–2), 184–192.
Surovoĭ, A., Ivanov, V.T., Chepurkin, A.V., Ivaniushchenkov, V.N., Driagalin, N.N., 1988. Is the Arg-Gly-Asp sequence the site for foot-and-mouth disease virus binding with cell receptor? Bioorg. Khim. 14 (7), 965–968.
Sutmoller, P., 2003. The fencing issue relative to the control of foot-and-mouth disease. Ann. N. Y. Acad. Sci., 191–200.
Thomson, G.R., Vosloo, W., Esterhuysen, J.J., Bengis, R.G., 1992. Maintenance of foot and mouth disease virus in buffalo (*Syncerus caffer* Sparrman, 1979) in Southern Africa. Rev. Sci. Tech. Off. Int. Epiz. 11, 1097–1107.
Thomson, G.R., Vosloo, W., Bastos, A.D.S., 2003. Foot and mouth disease in wildlife. Virus Res. 91, 145–161.
Van Rensburg, H.G., Nel, L.H., 1999. Characterization of the structural-protein-coding region SAT 2 type foot-and-mouth disease virus. Virus Genes 19 (3), 229–233.
Van Rensburg, H.G., Henry, T., Mason, P.W., 2004. Studies of genetically defined chimeras of a European type A virus and a South African Territories type 2 virus reveal growth determinants for foot-and-mouth disease virus. J. Gen. Virol. 85, 61–68.
Vosloo, W., Kirkbride, E., Bengis, R.G., Keet, D.F., Thomson, G.R., 1995. Genome variation in the SAT types of foot-and-mouth disease viruses prevalent in buffalo (Syncerus caffer) in the Kruger National Park and other regions of southern Africa, 1986–93. Epidemiol. Infect. 114, 203–218.
Vosloo, W., Bastos, A.D., Kirkbride, E., Esterhuysen, J.J., Janse van Rensburg, D., Bengis, R.G., Keet, D.F., Thomson, G.R., 1996. Persistent infection of African buffalo (*Syncerus caffer*) with SAT type foot-and-mouth disease viruses: rate of fixation of mutations, antigenic change and interspecies transmission. J. Gen. Virol. 77, 1457–1467.
Vosloo, W., Bastos, A.D., Michel, A., Thomson, G.R., 2001. Tracing movement of African buffalo in southern Africa. Rev. Sci. Tech. 20, 630–639.
Vosloo, W., Bastos, A.D.S., Sangare, O., Hargreaves, S.K., Thomson, G.R., 2003. Review of the status and control of foot and mouth disease in sub-Saharan Africa. Rev. Sci. Tech. Off. Int. Epiz. 21, 437–449.
Zhao, Q., Pacheco, J.M., Mason, P., 2003. Evaluation of genetically engineered derivatives of a chinese strain of foot-and-mouth disease virus reveals a novel cell-binding site which functions in cell culture and in animals. J. Virol. 77, 3269–3280.